

## A Compact High Gain Multiband Bowtie Slot Antenna with Miniaturized Triangular Shaped Metallic Ground Plane

Zaheer A. Dayo<sup>1</sup>, Qunsheng Cao<sup>1,\*</sup>, Yi Wang<sup>1</sup>, Permanand Soothar<sup>2</sup>, Imran A. Khoso<sup>1</sup>, Gulab Shah<sup>1</sup>, and Muhammad Aamir<sup>3</sup>

<sup>1</sup> College of Electronic and Information Engineering  
Nanjing University of Aeronautics and Astronautics, Nanjing, 211106, Peoples Republic of China  
zaheer.dayo, qunsheng, jflsjfls, shah\_hussain @nuaa.edu.cn; imrankhoso2@gmail.com

<sup>2</sup> School of Electronic and Optical Engineering  
Nanjing University of Science and Technology, Nanjing, 210094, Peoples Republic of China  
permanand.soothar@njust.edu.cn

<sup>3</sup> Department of Computer, Huanggang Normal University Huangzhou, Hubei, 438000, China, Peoples Republic of China  
aamirshaikh86@hotmail.com

**Abstract** — This paper presents a new compact, high gain and multiband planar bowtie slot antenna. The antenna structure comprises of dielectric substrate, copper conducting sheet, fillet triangular-shaped slots, and a chamfered metallic ground plane. The proposed antenna model is fed with the 50  $\Omega$  standard grounded coplanar waveguide (GCPW) feedline. The designed antenna is low profile with compact dimensions of  $0.379\lambda \times 0.186\lambda \times 0.012\lambda$  at 2.39 GHz frequency. Stable multi-resonant behavior of frequencies is obtained with the material selection, slots dimensions and position. Moreover, the parametric study has been carried out in order to validate the frequency tuning mechanism and impedance matching control. The novelty of designed antenna lies in high performance features which have been achieved with ultra-compact ( $0.039\lambda \times 0.022\lambda$ ) modified triangular shaped metallic ground plane. The proposed antenna is fabricated and experimentally verified. The antenna key features in terms of return loss, surface current distribution, peak gain, radiation efficiency and radiation patterns have been analyzed and discussed. The designed radiator exhibits the excellent performance including strong current density, peak realized gain of 6.3 dBi, 95% radiation efficiency, wide fractional bandwidth of 39.5% and good radiation characteristics at in-band frequencies. The simulation and measured results are in good agreement and hence make the proposed antenna a favorable candidate for the advanced heterogeneous wireless communication applications.

**Index Terms** — Advanced Heterogeneous Wireless Communication Applications, Bow-tie Slot Antenna, Compact, High Gain, Triangular shaped Ground Plane.

## I. INTRODUCTION

In past few decades, the demand to integrate multiple communication standards into a single device is increasing rapidly [1]. At present, different modern communication services are offered seamlessly by one device at the same time. Besides, there are multiple standards which can supports wireless local area network (WLAN), wireless fidelity (WIFI), world-wide interoperability over microwave access (WiMAX), global positioning systems (GPS), radio detection and ranging (RADAR) and satellite communication applications. It is important to design a system which can support multiple service standards and covers advanced heterogeneous applications including the civil and military regime [2]. Therefore, it is still a challenging task for active researchers to design a compact, multiband and high gain antenna with miniaturized triangular shaped metallic ground plane (MGP) specific for advanced heterogeneous wireless communication applications.

In the last five years, the researchers proposed several approaches and modified designs of slot antennas to achieve the multiband features. These approaches mainly focused on the different feeding networks [3],[4],[5], etching out slots from the radiating patch [6],[7],[8], defected ground structure (DGS) [9]–[11], artificial magnetic conductor (AMC) loaded lattice [12], complementary split ring resonator (CSRR) loaded metamaterial cell geometry [13],[14],[15] and fractal structures [16]. A dual-band antenna with cavity backed substrate integrated waveguide (SIW) approach has been reported [17]. The authors proposed annular ring slot antenna, which exhibited narrowband features [18]. A reconfigurable slot antenna with gamma shaped slots and

PIN diodes for different applications has been suggested [19]. A tapered slot antenna (TSA) array reported the optimal performance with increased the number of radiating elements [20]. These antennas have the complex geometries and operated at a given range.

Furthermore, the planar antennas with different configurations including U shaped slots and butterfly shaped parasitic elements [21], omega shaped strips cut out from rectangular slot [22], slotted inverted omega shaped MGP [23] and the single layer multi-element approach planar antennas have been reported [24]. The antennas achieved the different functions and cover multiple wireless communication applications. In the literature, antennas exhibited the dual-band triple-band and quad-band response [25],[26],[27] with reasonable performance. However, the suggested methods were complex and time consuming.

Recently, modified designs of multiband antennas have also been found in the literature. The authors designed the simple antennas with embedded slots on the radiator and obtained the penta-band and hexa-band response [28]. A comb-shaped slot antenna with simple configuration for penta-band applications was reported [29]. A simple antenna with cut slots was fabricated on Taconic material and obtained the penta-band response [30]. A multiband antenna for wireless handset covered lowest 6 GHz sub-band of fifth generation (5G) spectrum [31]. A crossed line based rectangular ring shaped multiband antenna fabricated on the flexible Rogers substrate material [32]. A modified design of slot antenna achieved the penta-band response with 2.3 dBi peak gain [33]. The authors proposed a bowtie slot antenna (BTSA) over 2-16 GHz frequency range and intended radiator occupied 1800 mm<sup>2</sup> ample space [34]. Another multiband antenna resonated within 1-7 GHz exhibited the peak gain of 5.45 dBi [35]. A magneto-electric dipole antenna achieved the multiband response with 6.6 dBi gain operated within 1.5-7.5 GHz [36]. A planar antenna with the multi-circular shaped slotted substrate exhibited multiband response [37]. The antenna has larger size and the peak gain and radiation efficiency is not reported. It is worthy to note that the recent reported works on compact multiband radiators have complex geometries, larger dimensions and most of the designed antennas achieved optimal results over short frequency range. Also, it is well known fact that there is always a tradeoff between antenna performance characteristics with compact size, computational load and expensive material. Hence, it is hard to achieve optimal results with simple and compact geometry of radiators keeping in view with the tradeoff among the multiple features of the intended radiator.

The key contribution of this manuscript is explained as:

- ❖ The proposed structure validates a new geometrical structure of BTSA with compact

electrical size  $0.379\lambda \times 0.186\lambda \times 0.012\lambda$ , which constructs the more efficient model that not only accelerates the optimization process but also consumes less computational load.

- ❖ The defined variables have increased the flexibility in terms of frequency tuning and impedance matching controllability.
- ❖ The designed antenna operates over a broad frequency span of 2-18 GHz in contrast to most of the reported works which resonated at the short frequency range.
- ❖ For the first time, the modified ultra-compact triangular shaped metallic ground plane has been designed with the advantages of antenna miniaturized dimensions.
- ❖ The proposed antenna has the simple geometry and covers advanced heterogeneous wireless communication applications.
- ❖ Finally, antenna performance is examined and analyzed with recently published state-of-the-art existing works. The antenna exhibits broad fractional BW at required frequencies, peak realized gain of 6.3 dBi and excellent radiation efficiency performance of 95% which is higher than most of the previous investigated antenna designs.

In this paper, a new compact multiband BTSA structure with ultra-compact triangular shaped MGP and GCPW feedline is presented. The proposed antenna is realized on low cost FR4 epoxy thick substrate. The designed radiator exhibits penta-band response at 10 dB return loss. The antenna has achieved high-performance features including good fractional bandwidth (BW), high realized gain, excellent radiation efficiency, strong surface current distribution and stable far-field co-polarization and cross-polarization patterns across the standard planes. The design and simulation of the prototype have been carried out with high frequency structure simulator (HFSS) full wave electromagnetic solver based on the finite element method (FEM). The proposed antenna covers 5G spectrum, WLAN (2.3 - 3.4 GHz), H-band (6-7.35 GHz), X-band (8.4 - 12.5 GHz), military airborne, naval and land RADAR (9.8 - 10.8 GHz), Ku-band (14.9 - 5.59 GHz) and satellite (17.17 - 17.37 GHz) frequency standard bands. Results reveal that the proposed antenna is well suitable for advanced latest heterogeneous wireless communication applications.

## II. PROPOSED RADIATOR METHODOLOGY

The antenna development stages are shown in Figs. 1 (a)-(e). The proposed antenna model comprises of dielectric substrate, copper conducting sheet (CCS), triangular shaped slots, MGP and 50  $\Omega$  GCPW feeding structure. These elements are engraved on the top and bottom side of the low cost FR4 epoxy printed circuit

board (PCB) laminate material with the constant values of relative permittivity  $\epsilon_r = 4.4$  and dielectric loss tangent  $\delta = 0.02$ . The structure of proposed radiator from the top, bottom and lateral view perspective is shown in Figs. 1 (e)-(g). The methodology of intended radiator is mainly based on designing of triangular shaped slots and CPW feedline above the thick substrate. CCS is embedded on top of the substrate. The standard thickness value of the copper material is chosen as 0.035 mm.

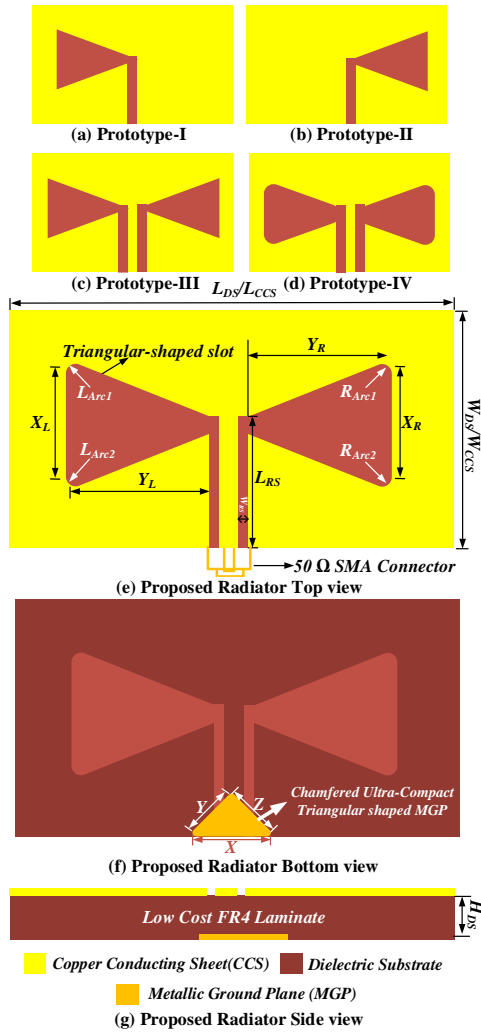


Fig. 1. Development stages of antenna and proposed radiator structure.

The triangular and rectangular slots are etched out from the upper CCS and form a left-side bowtie arm slot as depicted in Fig. 1 (a). Likewise, the right side triangular and rectangular slots are etched out from the upper CCS, which are exactly the mirror image of the left side bowtie arm slot and form right side bowtie arm slot as shown in Fig. 1 (b). The purpose of designing rectangular shaped slots is to realize the CPW feed line

as given in Fig. 1 (c). The dimensions of the feeding structure are carefully optimized to achieve the  $50 \Omega$  input impedance. Fillet operation is performed at top and bottom edges of the left and right ( $L_{Arc1,2} = R_{Arc1,2} = 0.0079\lambda$ ) triangular shaped bowtie arms. These two bowtie arm slots have fulfilled the symmetry property as illustrated in Fig. 1 (d). The miniaturized rectangular MGP with compact size of  $0.039\lambda \times 0.022\lambda$  is engraved on the bottom side of the dielectric substrate and right below the CPW feedline. The chamfered operation of  $0.0183\lambda$  is performed at the edges of MGP and thus forms ultra-compact triangular shaped MGP as shown in Fig. 1 (f). The proposed antenna possesses overall size of  $0.379\lambda \times 0.186\lambda \times 0.012\lambda$  (where  $\lambda$  denote free space wavelength at lowest resonant frequency of 2.39 GHz). An approximated equations extracted from transmission line model are used to compute the dimensions of the triangular shaped bowtie arms and CPW feedline [38].

The return loss performance of developed antenna prototypes is elucidated in Fig. 2. It can be analyzed that designed antenna structure obtained the fractional BW of 39.5%, 36.7%, 19.35%, 4.25% and 1.16% at third, first, second, fourth and fifth frequency bands. Likewise, good matching performance and stable penta-band resonances at targeted frequencies are observed.

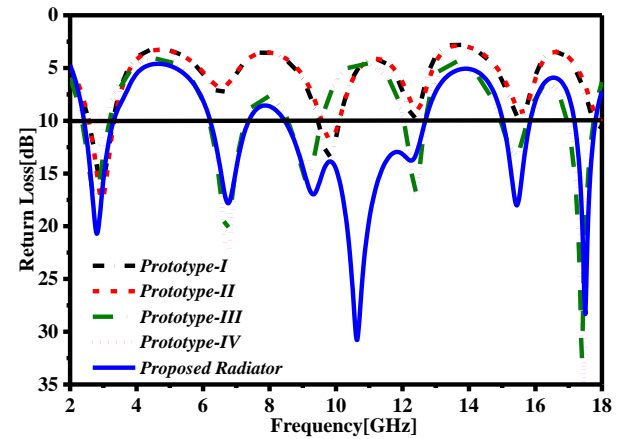


Fig. 2. Developed antenna model's return loss over specified frequency range.

Table 1: Antenna optimized values, unit: (mm)

Variable Symbol	Optimized Value	Variable Symbol	Optimized Value
$L_{DS}$	47.6	$L_{CCS}$	47.6
$W_{DS}$	23.4	$W_{CCS}$	23.4
$H_{DS}$	1.6	$X$	5
$X_L$	11.57	$Y$	2.3
$Y_L$	20	$Z$	2.3
$X_R$	11.57	$Y_R$	20
$W_{RS}$	1.2	$L_{RS}$	11.1

Further, the rectangular slots, dielectric substrate, CCS and MGP size (length and width) affects the proposed radiator performance. The chamfered and fillet operations are performed on the bowtie arm slots and MGP. This modification has the great impact on the multi-resonant performance and impedance matching control of the radiator. The proposed antenna exhibits overall optimum performance by carefully selecting defined variables values. The geometrical dimensions of the proposed antenna are listed in Table 1.

### III. SIMULATION RESULTS ANALYSIS

This section explains and analyzes the multi-resonant frequency tuning, matching performance, and surface current distribution of the proposed antenna.

#### A. Influence of $L_{RS}$ , $W_{DS}$ and $W_{CCS}$

Tuning of three bands is observed with the variation of three important variables as shown in Fig. 3. The multiple resonant bands centered at 2.86 GHz, 15.5 GHz and 17.5 GHz (first, fourth and fifth resonances) are tuned with the rectangular slot ( $L_{RS}$ ), dielectric substrate ( $W_{DS}$ ) and copper conducting sheet ( $W_{CCS}$ ) dimensions.

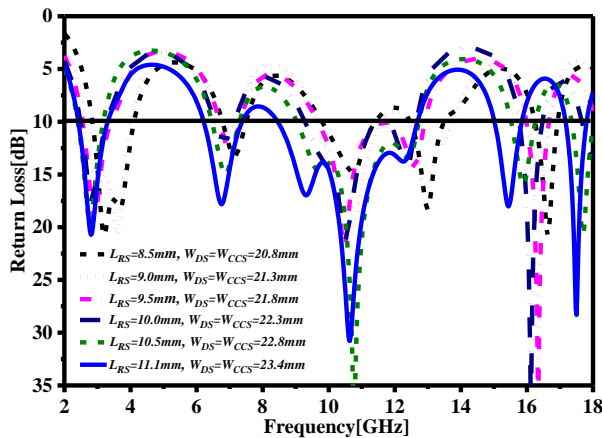


Fig. 3. Tuning and impedance matching control of multiple resonances across the operating frequency range.

It can be analyzed from Fig. 3 that the  $L_{RS}$  value varies from 8.5 mm to 11.1 mm with the step size of 0.5 mm and  $W_{DS}$ ,  $W_{CCS}$  values vary from 20.8 mm to 23.4 mm to achieve perfect matching at the higher values.

#### B. Influence of rectangular slot width ( $W_{RS}$ )

The influence of rectangular slot width ( $W_{RS}$ ) variation with step size of 0.2 mm across frequency is displayed in Fig. 4. One can observe shifting of the two bands centered at 6.72 GHz and 10.6 GHz (second and third) towards the lower and upper frequency range. As displayed in Fig. 4, optimum results are obtained at 1.2

mm which shows stable and good impedance matching over specified frequency.

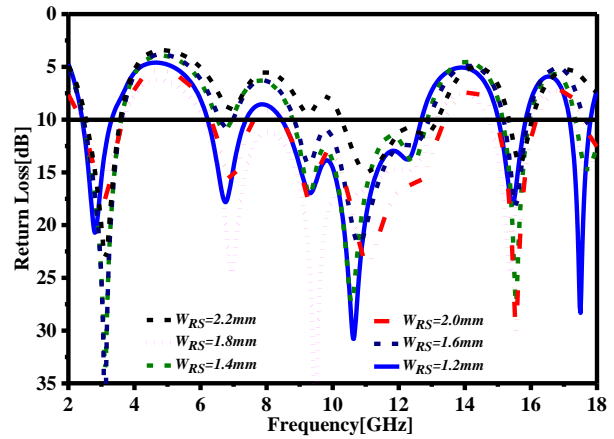


Fig. 4. Tuning and impedance matching control of resonances across the operating frequency range.

#### C. Influence of metallic ground plane (MGP)

The impact of MGP on overall performance of the proposed antenna is portrayed in Fig. 5. This impact is analyzed by simple MGP, chamfered MGP and absence of embedded MGP scenarios. One can observe that the antenna achieves required stable multiband response with chamfered MGP.

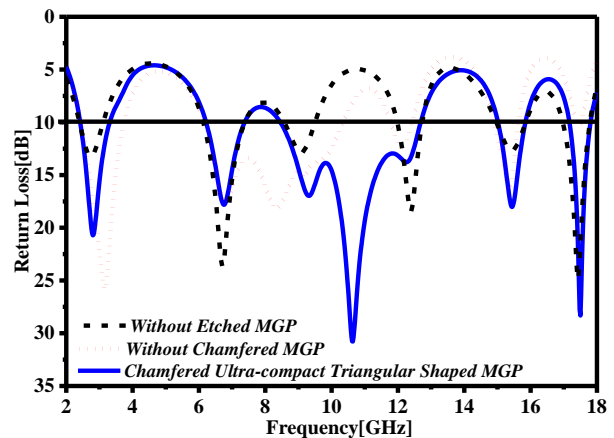


Fig. 5. Impact of chamfered MGP on the impedance matching across the frequency span.

#### D. Influence of different substrate material

In order to technically validate the stable multiband response, it is essential to verify the proposed radiator performance with different substrate material. The results of substrate materials are compared and depicted in Fig. 6. One can observe that the antenna achieves the perfect matching with stable desired resonances at 10 dB return loss by using the FR4 substrate material.

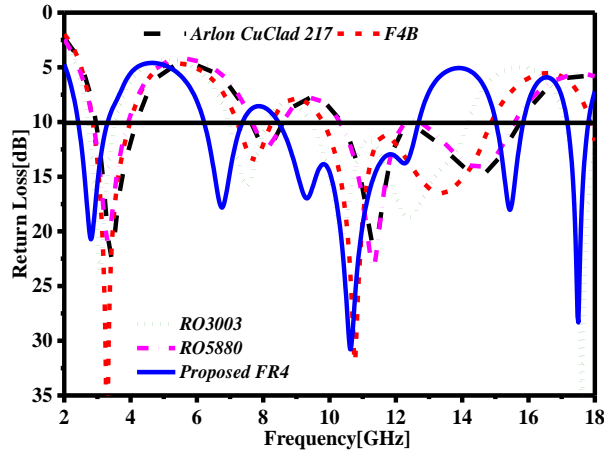


Fig. 6. Simulated results of different substrate material correspond to specified frequency.

**E. Surface current distribution (Jsurf)**

The concentration of current across the surface of radiator is analyzed and discussed in order to validate the effective working of proposed antenna. The current distributed density across the proposed antenna lattice at multiple resonant frequencies is depicted in Figs. 7 (a)-(e). It can be seen that at lower resonances i.e. 2.86 GHz and 6.72 GHz, the strong current is concentrated along the structure of the radiator and 50 Ω GCPW feedline. However, a diminutive variation in circulation of current at higher resonances for example, 10.6 GHz, 15.5 GHz and 17.5 GHz, can be noticed on the upper and lower front edges of radiator. The above analysis concludes that the current is equally distributed across the proposed antenna structure which confirms the cabinet’s optic principle for slot antennas.

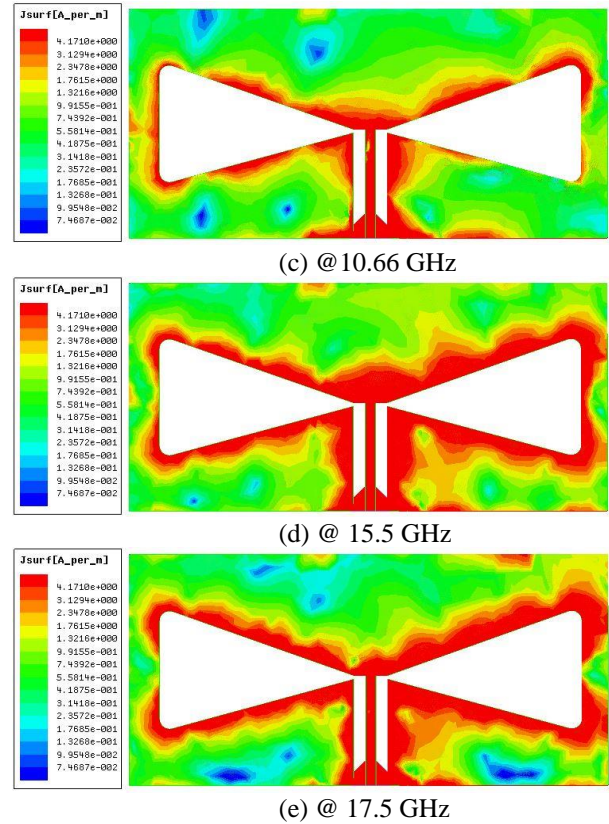
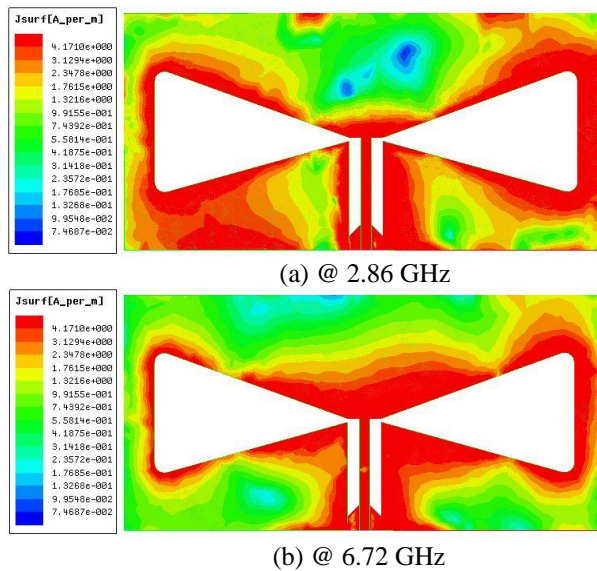


Fig. 7. Surface current distribution (Jsurf) across the proposed antenna lattice at multiple resonances.

**IV. EXPERIMENTALLY VALIDATED RESULTS**

This section mainly focuses on the experimental results of return loss, peak realized gain, radiation efficiency and co-polarization and cross-polarization far-field two dimensional (2D) radiation patterns. The fabricated antenna sample photograph along with top and bottom view is shown in Figs. 8 (a)-(b). The pin (inner conductor) of 50 Ω SMA connector is carefully soldered at middle of the GCPW feedline, which is engraved on top of the substrate. The outer conductor is connected to the chamfered ultra-compact triangular shaped MGP, which is embedded on the bottom of substrate as shown in Fig. 8 (b).

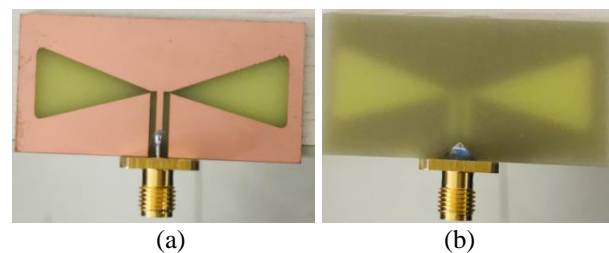


Fig. 8. Fabricated sample of the proposed radiator: (a) top view and (b) bottom view.

### A. Return loss performance

The fabricated antenna model is tested to validate simulation results. The simulated (blue) and measured (dashed red) return loss results across the specified frequency range are compared in Fig. 9. The antenna model is connected to one port of calibrated key sight PNA-X N-5245B network analyzer.

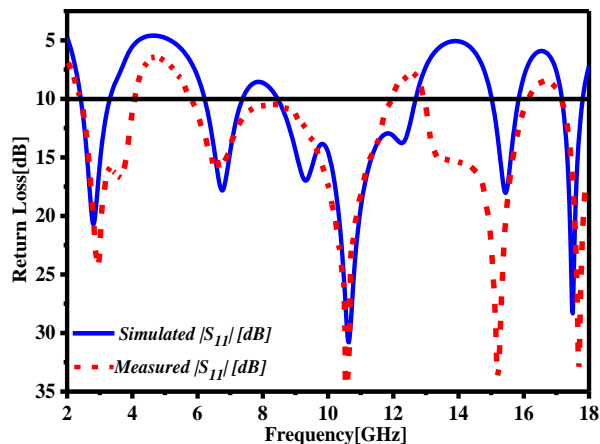


Fig. 9. Simulated and measured return loss performance across the operable frequency range.

It can be seen from Fig. 9 that the return loss performance of the designed and fabricated model is well coincides. One can observe a slight shift of the resonances in the measured result. A close agreement is clearly seen among the simulated and tested results. However, the deviation in experimental and simulation results is mainly due to the fabrication tolerances in the manufacturing of the substrate material, thickness, loss tangent or relative permittivity values, and imperfect soldering.

### B. Peak realized gain and radiation efficiency

The simulated and measured results of peak realized gain and radiation efficiency against the given frequency range are plotted and compared in Fig. 10. The antenna model simulation result (blue) achieved the high gain of 6.3 dBi and 5.72 dBi at 15.5 GHz and 17.5 GHz. Similarly, fair and acceptable gain is observed at other resonances. The peak realized gain of fabricated sample of antenna was measured with two identical ridge horn antennas with known gain. It can be seen from Fig. 10 (dashed red streak) that about 1 dB deviation in measured and simulated gain results is observed which validates the performance of fabricated prototype. The radiation efficiency simulation result of the proposed antenna model (black curve) shows high performance of 95%, 90%, 88%, 75.4% and 74.9% at in-band frequencies. An effective pattern integration method was applied to measure the radiation efficiency. The proposed antenna radiation efficiency measurement

results are slightly deviated in comparison with the simulation results as can be seen from Fig. 10 (dashed pink streak). The results have revealed the practical performance of designed sample across the operational frequency span.

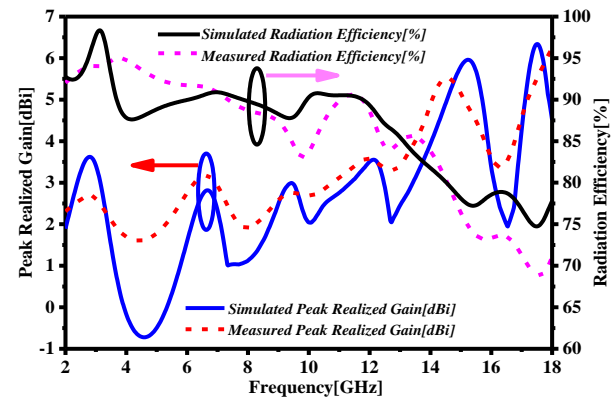


Fig. 10. Simulated and measured peak realized gain and radiation efficiency against the operable frequency range.

### C. Co-polar and cross polar patterns

The radiation patterns in principal planes of the proposed antenna are measured inside the anechoic chamber under far-field condition. The placement of device under test (DUT) is shown in Figs. 11 (a)-(b). The fabricated antenna prototype co-polarization and cross-polarization radiation patterns in elevation (E-plane) and azimuth (H-plane) are measured inside the chamber room. The measurement indoor facility walls are covered with radio absorbing material. DUT was placed on the azimuth rotator and move around 360°. The rotary table has been controlled by the positioner controller and connected to the computer with ethernet cable. The standard ridge gap horn (transmitter) and the DUT (receiver) have been fixed in line of sight (LoS) at a certain distance which fulfilled the far-field condition. Besides, the microwave cables are connected to the antennas and with the ports of vector network analyzer (VNA). A computer has been installed to monitor the measurement results, execute the commands and save the measured data.

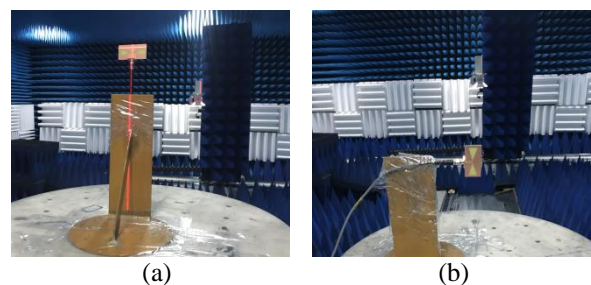


Fig. 11. DUT placement in anechoic chamber.

The simulation and measurement results of co-polarization and cross-polarization in principal planes at in-band resonances are displayed and compared in Figs. 12 (a)-(j). The co-polarization and cross-polarization pattern results of the proposed antenna in E-plane at multiple resonances are shown in Figs. 12 (a), (c), (e), (g) and (i). The antenna exhibits near omni-directional radiation pattern of co-polarization in E-plane at in-band resonances. One can see the simulation results at higher resonances are changing gradually. At higher resonances cross-polarization level is slightly increased. The cross-polarization level is almost -20 dB at targeted resonances. It is found that the measurement results of co-polarization and cross-polarization radiation patterns are slightly deteriorated as the frequency increases and nulls are observed at higher resonances. Further, the co-polarization and cross-polarization antenna results in H-plane at multiple resonances are portrayed in Figs. 12 (b), (d), (f), (h) and (j). The antenna exhibits nearly monopole like co-polarization and cross-polarization radiation pattern at lower resonances. A slight change in radiation patterns at higher resonances is observed. One can analyze that the simulation and measurement results show a diminutive shift and slightly deteriorated. The deviations in measured results at principal planes are mainly due to the fact of losses inside measurement chamber facility, rotation of the antenna model and SMA radiation. The overall measured radiation patterns at in-band resonant frequencies are well coincide with simulated results.

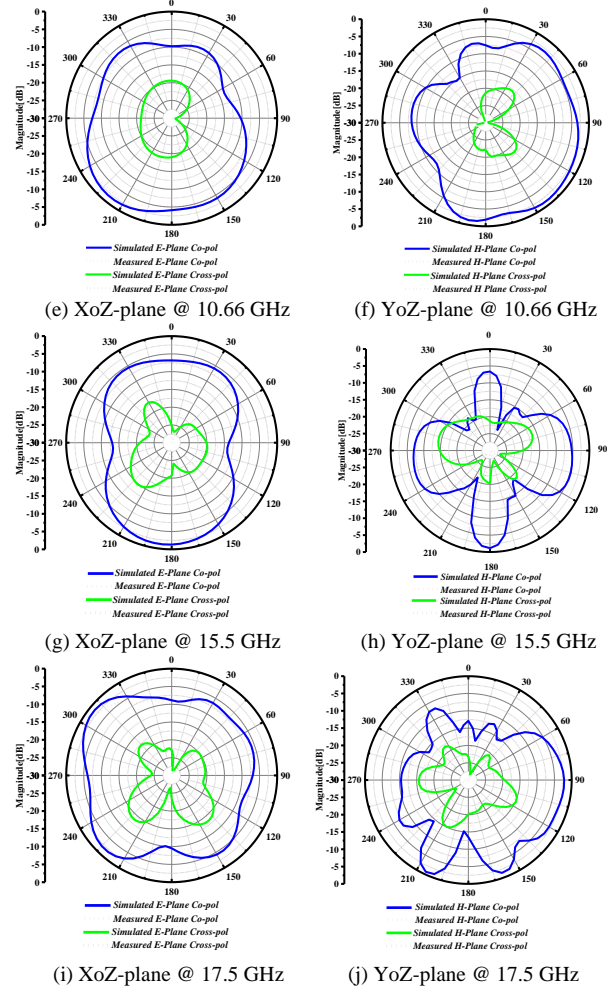
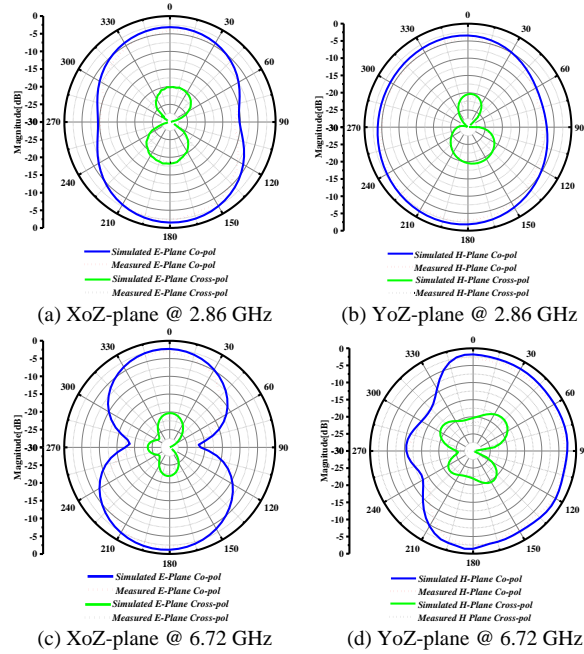


Fig. 12. Simulated and measured co-polar and cross-polar far-field patterns across the principal plane at multiple resonances.

## V. LITERATURE COMPARISON

The performance comparison of the proposed antenna with state-of-the-art work is compared in Table II. It can be seen that the proposed antenna is miniaturized, low profile and exhibited the optimal performance in terms of peak gain and radiation efficiency. The proposed antenna is very smaller in size and decreases in overall occupied space of 84.5%, 38.1% and 36.34% in comparison to Refs. [29]-[31]. The antenna reported in [29] obtained a higher gain with compromised overall occupied space. It can be noticed that the radiation efficiency of the antennas were not focused in [5], [33] and [35]-[37]. From the comparison analyzed results, it is evident that most of the reported works on multiband antennas cover a small frequency

span as compared to the proposed multiband BTSA.

Table 2: Proposed radiator performance comparison with state-of-the-art investigated multiband antennas

Ref.	Electrical Size ( $\lambda$ ) [ $L_{DS} \times W_{DS}$ ] (mm <sup>2</sup> )	Antenna Profile ( $\lambda$ ) [ $H_{DS}$ ] (mm)	Gain (dBi)	Efficiency (%)
<b>Our work</b>	0.379 $\lambda$ ×0.186 $\lambda$	0.012 $\lambda$	6.3	95
[29]	0.694 $\lambda$ ×0.484 $\lambda$	0.003 $\lambda$	6.46	79
[30]	0.53 $\lambda$ ×0.48 $\lambda$	0.009 $\lambda$	5.37	94.8
[31]	0.966 $\lambda$ ×0.485 $\lambda$	0.013 $\lambda$	2.86	77
[33]	0.966 $\lambda$ ×0.485 $\lambda$	0.004 $\lambda$	2.5	Not Reported (NR)
[5]	0.099 $\lambda$ ×0.165 $\lambda$	0.0135 $\lambda$	3.0	NR
[35]	0.35 $\lambda$ ×0.22 $\lambda$	0.0079 $\lambda$	5.45	NR
[36]	0.4 $\lambda$ ×0.13 $\lambda$	0.16 $\lambda$	6.6	NR
[37]	0.489 $\lambda$ ×0.351 $\lambda$	0.024 $\lambda$	NR	NR

## VI. CONCLUSION

In this article, a new compact high gain and multiband BTSA with miniaturized triangular shaped MGP has been proposed and investigated. The antenna is realized on the low-cost FR4 epoxy thick substrate. The antenna prototype has miniaturized dimensions of 0.379 $\lambda$ ×0.186 $\lambda$ ×0.012 $\lambda$ . Influence of multiple variables have been analyzed and discussed. Analysis of surface current distribution at multiple resonances has been investigated. The proposed antenna model exhibited an excellent performance of return loss, peak realized gain, radiation efficiency and stable far-field co-polarization and cross-polarization radiation patterns. The designed antenna obtained the wide fractional bandwidths at in-band resonances. High gain of 6.3 dBi, 5.72 dBi, 3.64 dBi, 2.89 dBi and 2.58 dBi are achieved at 17.5 GHz, 15.5 GHz, 2.86 GHz, 6.72 GHz and 10.66 GHz resonances. The proposed antenna showed an excellent radiation efficiency performance of 95%, 90%, 88%, 75.5% and 74.9% at in-band frequencies. The designed antenna has been fabricated, tested and experimentally verified. The simulation and measured results are in close agreement and hence make the proposed antenna as an excellent choice for advanced heterogeneous wireless communication applications.

## ACKNOWLEDGMENT

Authors Zaheer Ahmed Dayo, Qunsheng Cao, Yi Wang and Gulab Shah gratefully acknowledge the support from National Natural Science Foundation of China under grant No. 61871219.

## REFERENCES

- [1] E. A. Soliman, S. Brebels, P. Delmotte, G. A. E. Vandenbosch, and E. Beyne, "Bow-tie slot antenna

fed by CPW," *Electron. Lett.*, vol. 35, no. 7, pp. 514-515, Apr. 1999.

- [2] Z. A. Dayo, Q. Cao, Y. Wang, S. Ur Rahman, and P. Soothar, "A compact broadband antenna for civil and military wireless communication applications," *Int. J. Adv. Comput. Sci. Appl.*, vol. 10, no. 9, pp. 39-44, Sep. 2019.
- [3] S. C. Basaran and K. Sertel, "Compact and planar monopole antenna for WLAN and WiMAX applications," *Appl. Comput. Electromagn. Soc. J.*, vol. 30, no. 5, pp. 546-550, May 2015.
- [4] P. Soothar, H. Wang, C. Xu, Z. A. Dayo, B. Muneer, and K. Kanwar, "A compact broadband and high gain tapered slot antenna with stripline feeding network for H, X, Ku and K band applications," *Int. J. Adv. Comput. Sci. Appl.*, vol. 11, no. 7, pp. 239-244, July 2020.
- [5] P. N. VummadiSETTY and A. Kumar, "Multi feed multi band uniplanar ACS fed antenna with N shape and inverted L shape radiating branches for wireless applications," *Microsyst. Technol.*, vol. 24, no. 4, pp. 1863-1873, Apr. 2018.
- [6] K. Mondal, P. P. Sarkar, and D. Chanda Sarkar, "High gain triple band microstrip patch antenna for WLAN, Bluetooth and 5.8 GHz/ISM band applications," *Wirel. Pers. Commun.*, vol. 109, no. 4, pp. 2121-2131, Dec. 2019.
- [7] A. Ahmad, F. Arshad, S. I. Naqvi, Y. Amin, and H. Tenhunen, "Design, fabrication, and measurements of extended I-shaped multiband antenna for wireless applications," *Appl. Comput. Electromagn. Soc. J.*, vol. 33, no. 4, pp. 388-393, Apr. 2018.
- [8] M. R. Ahsan, M. T. Islam, and M. Habib Ullah, "A new meandered-stripline fed dual band patch antenna," *Appl. Comput. Electromagn. Soc. J.*, vol. 30, no. 2, pp. 213-221, Feb. 2015.
- [9] M. M. Fakharian, P. Rezaei, and A. A. Orouji, "A novel slot antenna with reconfigurable meander-slot DGS for cognitive radio applications," *Appl. Comput. Electromagn. Soc. J.*, vol. 30, no. 7, pp. 748-753, July 2015.
- [10] D. Behera, B. Dwivedy, D. Mishra, and S. K. Behera, "Design of a CPW fed compact bow-tie microstrip antenna with versatile frequency tunability," *IET Microwaves, Antennas Propag.*, vol. 12, no. 6, pp. 841-849, May 2018.
- [11] C. Zebiri, D. Sayad, I. Elfergani, A. Iqbal, W. F. A Mshwat, J. Kosha, J. Rodriguez, R. Abd-Alhameed, "A compact semi-circular and arc-shaped slot antenna for heterogeneous RF front-ends," *Electron.*, vol. 8, no. 10, Oct. 2019.
- [12] E. W. Coetzee, J. W. Odendaal, and J. Joubert, "A quad-band antenna with AMC reflector for WLAN and WiMAX applications," *Appl. Comput. Electromagn. Soc. J.*, vol. 33, no. 10, pp. 1123-1128, Oct. 2018.

- [13] R. Rajkumar and K. Usha Kiran, "A compact meta-material multiband antenna for WLAN/WiMAX/ITU band applications," *AEU - Int. J. Electron. Commun.*, vol. 70, no. 5, pp. 599-604, May 2016.
- [14] S. I. R. and S. Raghavan, "CSRR-based compact pentaband printed antenna for GPS/GSM/ WLAN/WiMAX applications," *Microw. Opt. Technol. Lett.*, vol. 57, no. 7, pp. 1538-1542, July 2015.
- [15] Z. A. Dayo, Q. Cao, P. Soothar, M. M. Lodro, and Y. Li, "A compact coplanar waveguide feed bow-tie slot antenna for WIMAX, C and X band applications," *2019 IEEE Intl. Conf. on Comput. Electromagn.*, (ICCEM), Shanghai, China, pp. 1-3, July 2019.
- [16] N. Kumar Mungaru, K. Yogaprasad, and V. R. Anitha, "A quad-band Sierpinski based fractal antenna fed by co-planar waveguide," *Microw. Opt. Technol. Lett.*, vol. 62, no. 2, pp. 1-6, Oct. 2019.
- [17] M. A. Belen, P. Mahouti, A. Çaliskan, and A. Belen, "Modeling and realization of cavity-backed dual band SIW antenna," *Appl. Comput. Electromagn. Soc. J.*, vol. 32, no. 11, pp. 974-978, Nov. 2017.
- [18] Y. F. Lin, Y. C. Kao, S. C. Pan, and H. M. Chen, "Bidirectional radiated circularly polarized annular-ring slot antenna for portable RFID reader," *Appl. Comput. Electromagn. Soc. J.*, vol. 25, no. 3, pp. 182-189, Mar. 2010.
- [19] B. Badamchi, A. Valizade, P. Rezaei, and Z. Badamchi, "A reconfigurable square slot antenna with switchable single band, UWB and UWB with band notch function performances," *Appl. Comput. Electromagn. Soc. J.*, vol. 29, no. 5, pp. 383-390, May 2014.
- [20] P. Soothar, H. Wang, B. Muneer, Z. A. Dayo, and B. S. Chowdhry, "A broadband high gain tapered slot antenna for underwater communication in microwave band," *Wirel. Pers. Commun.*, vol. 116, no. 2, pp. 1025-1042, Jan. 2021.
- [21] P. Beigi, J. Nourinia, B. Mohammadi, and A. Valizade, "Bandwidth enhancement of small square monopole antenna with dual band notch characteristics using U-shaped slot and butterfly shape parasitic element on backplane for UWB applications," *Appl. Comput. Electromagn. Soc. J.*, vol. 30, no. 1, pp. 78-85, Jan. 2015.
- [22] A. Valizade, C. Ghobadi, J. Nourinia, N. Ojaroudi, and M. Ojaroudi, "Band-notch slot antenna with enhanced bandwidth by using  $\Omega$ -shaped strips protruded inside rectangular slots for UWB applications," *Appl. Comput. Electromagn. Soc. J.*, vol. 27, no. 10, pp. 816-822, Oct. 2012.
- [23] Z. A. Dayo, Q. Cao, Y. Wang, P. Soothar, B. Muneer, and B. S. Chowdhry, "A compact broadband high gain antenna using slotted inverted omega shape ground plane and tuning stub loaded radiator," *Wirel. Pers. Commun.*, vol. 113, no. 1, pp. 499-518, July 2020.
- [24] Z. A. Dayo, Q. Cao, Y. Wang, S. Pirbhulal, and A. H. Sodhro, "A compact high-gain coplanar waveguide-fed antenna for military RADAR applications," *Int. J. Antennas Propag.*, vol. 2020, no. 8024101, pp. 1-10, Aug. 2020.
- [25] D. Pathak, S. K. Sharma, and V. S. Kushwah, "Dual-band linearly polarized integrated dielectric resonator antenna for Wi-MAX applications," *Wirel. Pers. Commun.*, vol. 111, no. 1, pp. 235-243, Mar. 2020.
- [26] K. Yu, Y. Li, and W. Yu, "A compact triple band antenna for bluetooth, WLAN & WiMAX applications," *Appl. Comput. Electromagn. Soc. J.*, vol. 32, no. 5, pp. 424-429, May 2017.
- [27] S. S. Sran and J. S. Sivia, "Quad staircase shaped microstrip patch antenna for S, C and X band applications," *Procedia Comput. Sci.*, vol. 85, pp. 443-450, Feb. 2016.
- [28] K. Srivastava, A. Kumar, and B. K. Kanaujia, "Design of compact penta-band and hexa-band microstrip antennas," *Frequenz*, vol. 70, no. 3-4, pp. 101-111, Mar. 2016.
- [29] Y. J. Chen, T. W. Liu, and W. H. Tu, "CPW-fed penta-band slot dipole antenna based on comb-like metal sheets," *IEEE Antennas Wirel. Propag. Lett.*, vol. 16, pp. 202-205, May 2017.
- [30] N. H. Gad and M. Vidmar, "Design of a microstrip-fed printed-slot antenna using defected ground structures for multiband applications," *Appl. Comput. Electromagn. Soc. J.*, vol. 33, no. 8, pp. 854-860, Aug. 2018.
- [31] A. J. Khalilabadi and A. Zadehghol, "Multiband antenna for wireless applications including GSM/UMTS/LTE and 5G bands," *Appl. Comput. Electromagn. Soc. J.*, vol. 34, no. 2, pp. 270-271, Feb. 2019.
- [32] A. Javed, A. Ejaz, S. Mehak, Y. Amin, J. Loo, and H. Tenhunen, "Miniaturized cross-lines rectangular ring-shaped flexible multiband antenna," *Appl. Comput. Electromagn. Soc. J.*, vol. 34, no. 5, pp. 625-630, May 2019.
- [33] B. Bag, P. Biswas, S. Biswas, P. P. Sarkar, and D. Ghoshal, "Novel monopole microstrip antennas for GPS, WiMAX and WLAN applications," *J. Circuits, Syst. Comput.*, vol. 29, no. 3, pp. 1-15, May 2020.
- [34] Z. A. Dayo, Q. Cao, Y. Wang, and P. Soothar, "A compact high gain multiband bow-tie slot antenna," *2019 Int. Appl. Comput. Electromagn. Soc. Symp. - China (ACES)*, Nanjing, China, pp. 1-2, Apr. 2019.
- [35] M. A. Al-Mihrab, A. J. Salim, and J. K. Ali, "A compact multiband printed monopole antenna with hybrid polarization radiation for GPS, LTE, and satellite applications," *IEEE Access*, vol. 8, pp.

- 110371-110380, June 2020.
- [36] G. Yang, S. Zhang, J. Li, Y. Zhang, and G. F. Pedersen, "A multi-band magneto-electric dipole antenna with wide beam-width," *IEEE Access*, vol. 8, pp. 68820-68827, Apr. 2020.
- [37] A. E. Ahmed and W. A. E. Ali, "A Novel multiband antenna with 3D-printed multicircular substrate for wireless applications," *2nd Int. Conf. Electr. Commun. Comput. Eng. ICECCE 2020*, pp. 1-5, Aug. 2020.
- [38] R. Nayak and S. Maiti, "A review of bow-tie antennas for GPR applications," *IETE Tech. Rev. (Institution Electron. Telecommun. Eng. India)*, vol. 36, no. 4, pp. 382-397, July 2019.



**Zaheer Ahmed Dayo** was born in village Rustam, District Shikarpur Sindh, Pakistan. He received the M.E degree in Telecommunication Engineering & Management from Mehran University of Engineering & Technology (MUET) Jamshoro Sindh Pakistan in the year 2014.

He is currently pursuing the Ph.D. degree under the supervision of Professor Qunsheng Cao; with major in Communication Information System, at College of Electronic and Information Engineering (CEIE), Nanjing University of Aeronautics & Astronautics (NUAA), P.R China. Dayo has published several articles in international journals and conference proceedings. He served as a reviewer and TPC member in international journal and conference He has a vast academic and research experience of more than 5 years. He is currently working in the field of Electromagnetics particularly focused on Microwave & RF Engineering and Measurements areas. His current research interests include Designing of Compact, Broadband, High gain Antennas, Array topology and optimization Schemes, Multiband slot antennas, Reconfigurable, Metamaterial inspired antennas, Active and Passive Frequency Selective Surfaces.



**Qunsheng Cao** received the Ph.D. degree in Electrical Engineering from The Hong Kong Polytechnic University, Hong Kong, in 2000. From 2000 to 2005, He worked as a Research Associate with the Department of Electrical Engineering, University of Illinois at Urbana-Champaign and with the Army High Performance Computing Research Center, University of Minnesota, U.S.A. In 2006, he joined the Nanjing University of

Aeronautics and Astronautics, China, as a Professor for Electrical Engineering. He has authored more than 190 academic articles in refereed international journals and conference proceedings. His current research interests include computational electromagnetics, microwave, and antennas technologies and radar signal processing. His research team is also engaged in high-speed circuit signal integrity, antenna, microwave components, and new method in radar signal processing.



**Yi Wang** received the B.S. and Ph.D. degrees in Communication and Information System from the Nanjing University of Aeronautics and Astronautics (NUAA), Nanjing, China, in 2006 and 2012, respectively. In 2012, he joined the College of Electronic and

Information Engineering, NUAA, as an Assistant Professor, where he is currently working as an Associate Professor. His research interests include computational electromagnetics, especially the finite difference time-domain (FDTD) method, the FDTD modeling of the entire earth-ionosphere system, and the earthquake electromagnetics, and research focuses on the FDTD simulation of anisotropic media and earthquake phenomena.



**Permanand Soothar** was born in Sindh, Pakistan. He received the M.E. degree in Electronics and Telecom Engineering from the Mehran University of Engineering and Technology (MUET), Jamshoro, Sindh Pakistan, in 2012. Soothar is working as a Faculty Member in the

Department of Electronics Engineering, MUET Jamshoro Since 2015. Currently, He is pursuing the Ph.D. degree under the supervision of Professor Hao Wang at the School of Electronic and Optoelectronic Engineering, Nanjing University of Science and Technology (NJUST), Nanjing, P.R. China. His research interests include planar microstrip patch antennas, Ultra-wideband antennas, Millimeter-wave antennas, 5G communication antennas, Gap waveguide technology, satellite communication system, dual polarization slotted waveguide antennas and Arrays.



**Imran A Khoso** received the M.S. degree in Information and Communication Engineering from University of Science and Technology Beijing, Beijing in 2019. He is currently working toward the Ph.D. degree in Communication and Information Systems at Nanjing University of

Aeronautics and Astronautics, Nanjing, China. Khoso serves as a peer reviewer for IEEE Access, IET Communications, and several conferences. His research interests include random matrix theory, signal processing and wireless communications.



**Gulab Shah** received his M.Sc. and M.Phil. degrees in the field of Electronics from Quaid-e- Azam University (QAU), Islamabad, Pakistan in 2006 and 2008, respectively. Currently, Shah is pursuing Ph.D. degree from College of Electronic and Information

Engineering Nanjing University of Aeronautics and Astronautics, China. His research interests include radio frequency and microwave designing components, antennas, meta-material and frequency selective surface.



**Muhammad Aamir** received the Bachelor of Engineering degree in Computer Systems Engineering from Mehran University of Engineering & Technology Jamshoro, Sindh, Pakistan, in 2008, the Master of Engineering degree in Software Engineering from Chongqing University, China, in 2014, and the Ph.D. degree in Computer Science and Technology from Sichuan University, Chengdu, China, in 2019. He is currently an Associate Professor at the Department of Computer, Huanggang Normal University, Huanggang, China. His main research interests include pattern recognition, computer vision, image processing, deep learning, wireless communication and fractional calculus.